Accepted Manuscript

Discovery of dual GyrB/ParE inhibitors active against Gram-negative bacteria

Ho Soo Yei, Wang Weiling, Ng Fui Mee, Wong Yun Xuan, Poh Zhi Ying, Tan Sum Wai Eldwin, Ang Shi Hua, Liew Si Si, Joyner Wong Yin Sze, Yvonne Tan, Anders Poulsen, Vishal Pendharkar, Kanda Sangthongpitag, John Manchester, Gregory Basarab, Jeffrey Hill, Thomas H. Keller, Joseph Cherian

PII: S0223-5234(18)30689-5

DOI: 10.1016/j.ejmech.2018.08.025

Reference: EJMECH 10636

To appear in: *European Journal of Medicinal Chemistry*

Received Date: 7 May 2018

Revised Date: 3 August 2018

Accepted Date: 10 August 2018

Please cite this article as: H.S. Yei, W. Weiling, N.F. Mee, W.Y. Xuan, P.Z. Ying, T.S. Wai Eldwin, A.S. Hua, L.S. Si, J.W. Yin Sze, Y. Tan, A. Poulsen, V. Pendharkar, K. Sangthongpitag, J. Manchester, G. Basarab, J. Hill, T.H. Keller, J. Cherian, Discovery of dual GyrB/ParE inhibitors active against Gram-negative bacteria, *European Journal of Medicinal Chemistry* (2018), doi: 10.1016/j.ejmech.2018.08.025.

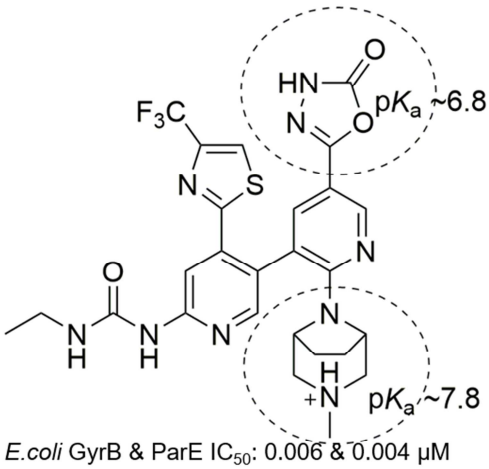

E.coli GyrB & ParE IC_{50}: 0.006 & 0.004 μM

P.aeruginosa, *E.coli* and *A. baumannii* MIC: 2.4 - 0.5 μg/mL

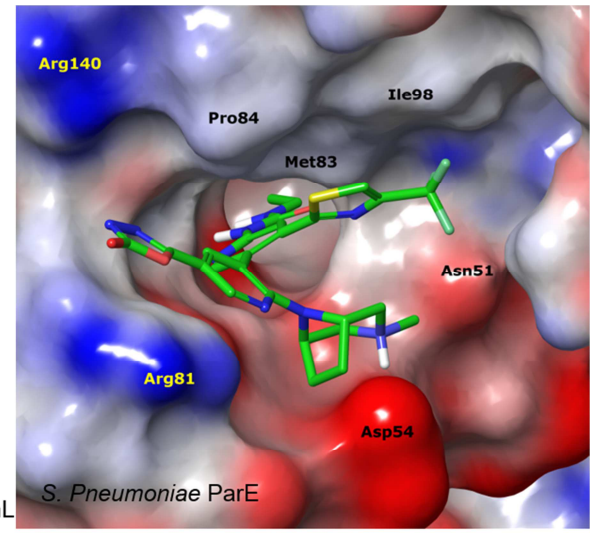

Discovery of dual GyrB/ParE inhibitors active against Gram-negative bacteria

Ho Soo Yei,[a] Wang Weiling,[a] Ng Fui Mee,[a] Wong Yun Xuan,[a] Poh Zhi Ying,[a] Tan Sum Wai Eldwin,[a] Ang Shi Hua,[a] Liew Si Si,[a] Joyner Wong Yin Sze,[a] Yvonne Tan,[a] Anders Poulsen,[a] Vishal Pendharkar,[a] Kanda Sangthongpitag,[a] John Manchester,[b,1] Gregory Basarab,[b,1] Jeffrey Hill,[a] Thomas H. Keller,[a] Joseph Cherian [a,*]

[a] *Experimental Therapeutics Centre, 13 Biopolis Way, Nanos, Singapore 13866;*

[b] *AstraZeneca, 35 Gatehouse Dr, Waltham, MA 02451, USA.*

KEYWORDS: Gram-negative bacteria, dual target inhibition, Gyrase B, ParE, Gyrase, TopoIV.

ABSTRACT

Even though many GyrB and ParE inhibitors have been reported in the literature, few possess activity against Gram-negative bacteria. This is primarily due to limited permeability across Gram-negative bacterial membrane as well as bacterial efflux mechanisms. Permeability of compounds across Gram-negative bacterial membranes depends on many factors including physicochemical properties of the inhibitors. Herein, we show the optimization of pyridylureas leading to compounds with potent activity against Gram-negative bacterial species such as *P.aeruginosa, E.coli* and *A.baumannii*.

1. Introduction

Drug resistant Gram-negative bacterial infections pose a significant threat to people in healthcare settings and especially patients in intensive care units [1-3]. Unfortunately the

*Corresponding author. E-mail address: jcherian@etc.a-star.edu.sg (J. Cherian)
[1]Present address:
J. Manchester: Novartis Institutes for BioMedical Research, 250 Massachusetts Ave, Cambridge, MA 02139, USA.
G. Basarab: H3D, Department of Chemistry, PD Hahn Building, Upper Campus, University of Cape Town, Rondebosch 7700, South Africa.

prospects for new antibacterial agents are bleak and the fact that no new class of drugs with Gram-negative activity has been approved since 1987 illustrates the magnitude of the problem. Research and development efforts focused on next-generation β-lactam antibiotics resulted in the approval of two new cephalosporin / β-lactamase inhibitor combinations [4, 5]. However the combination partners of the new cephalosporins in these therapies are not very effective against several β-lactamases underlining the urgent need for antibacterial agents with a novel mechanism of action [6-8]. Because the emergence of resistance against single agents is rapid, antibacterial agents that inhibit multiple targets are preferred as they are known to have lower frequency of resistance [9].

The ATPase domain containing subunits of bacterial DNA Gyrase and TopoisomeraseIV, Gyrase B and ParE, respectively, have long been recognized as antibacterial targets. While there are several known inhibitors of GyrB and ParE [10-20], none have been approved for clinical use. Inhibitors of these enzymes would qualify as dual target inhibitors thus potentially reducing frequency of resistance. A majority of the known GyrB/ParE inhibitors possess Gram- positive activity with limited or no activity against Gram-negative bacteria.

Being cytoplasmic targets, potential inhibitors of these enzymes have to cross the asymmetric outer membrane, the periplasmic space and finally the inner membrane to reach the targets in Gram-negative bacteria [21, 22]. In addition to these permeability challenges, Gram-negative bacteria have efficient efflux mechanisms for the removal of antibacterial agents from the cytoplasm.

When analyzing the challenges of designing dual GyrB/ParE inhibitors for Gram-negative bacteria, three issues stand out. First, molecules must show potent inhibition on both enzymes. It has been reported that inhibition of GyrB alone only slowed down DNA replication as ParE could support replication in *Escherichia coli* [23]. Inhibition of both GyrB and ParE was required to stop DNA replication rapidly [23]. Second, many reported

GyrB/ParE inhibitors are optimized on Gram-positive enzyme targets and therefore exhibit good activity on Gram-positive bacteria. While there is high sequence homology in the ATPase domain of these enzymes, small changes in amino acid sequence [24] make designing inhibitors that are active on both targets across Gram-positive and -negative bacterial species very challenging. Third, the unique structure of the Gram-negative cell wall, as well as the presence of efflux mechanisms, calls for optimal physicochemical properties for a given compound to show an antibacterial effect [25, 26].

The tricyclic inhibitor class represented by compound **1** [16] is an example of a potent inhibitor of both Gram-negative GyrB and ParE showing good antibacterial activity. So far this level of a Gram-negative activity has not been achieved with the pyridyl urea scaffold. A recent publication [27] has shown the evolution of a pyridyl urea fragment into compound **2** and **3** which are potent *E.coli* GyrB inhibitors but are >100 fold less active against *E.coli* ParE. Herein, we show that by achieving potent dual target inhibition and optimizing pK_a, it is possible to achieve compounds having MIC_{90}s against Gram-negative species such as *Pseudomonas aeruginosa* and *Acinetobacter baumannii* in the low µg/mL range.

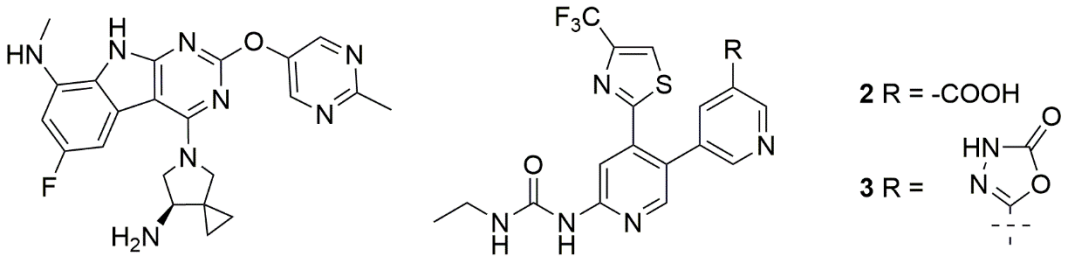

1

Fig. 1. Representative tricyclic pyrimidoindole and pyridylurea based GyrB/ParE dual inhibitors.

2. Chemistry:

Scheme 1 shows synthesis of compounds **6**, **11** and **12**. Suzuki coupling reaction between **4** and previously known boronic acid **5** [27] gave compound **6**.

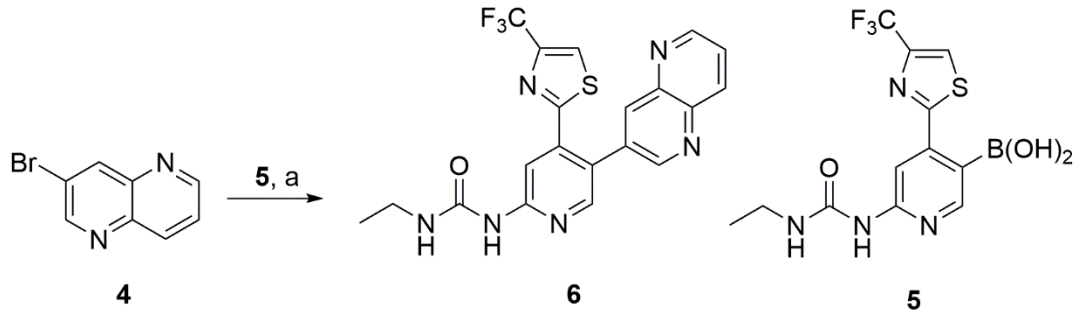

Scheme 1. *Reagents and conditions:* (a) aq. K_3PO_4, Pd(dppf)Cl_2.DCM, 1,4-dioxane, 100 ^oC, 16 h.

Nucleophilic displacement of the chloro group in **7** with amines **8**–**13** and subsequent Suzuki coupling with **5** gave compounds **14**–**20** (scheme 2). Removal of *N*-boc protection in **17**–**20** using TFA in DCM gave rise to **21**–**24**.

In a similar way, intermediates **27**–**29** (scheme 3) were synthesized from **25** and **26** by nucleophilic displacement of chlorine with amines **8, 9** and **12** in DMF in presence of K_2CO_3.

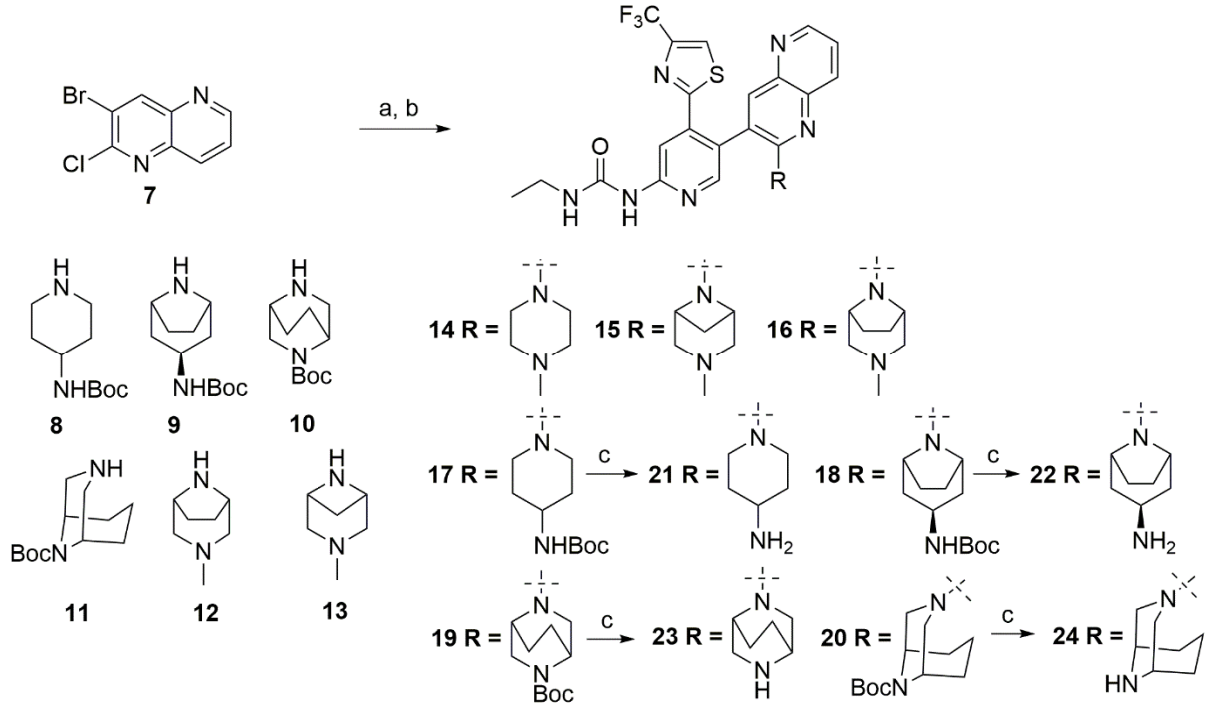

Scheme 2. *Reagents and conditions:* (a) DMF, K_2CO_3, amine, 80 ^oC, 12 h; (b) **5**, aq. K_3PO_4, Pd(dppf)Cl_2.DCM, 1,4-dioxane, 100 ^oC, 16 h; (c) CF_3CO_2H, CH_2Cl_2, rt, 4 h.

Suzuki coupling reaction between **5** and **27** and subsequent hydrolysis of the ester group resulted in compound **34**. HATU-mediated coupling of **34** with $MeSO_2NH_2$ in presence of trimethylamine gave compound **36**. Heating **12** with **32** at 80 ^oC in DMF and subsequent Suzuki coupling of the product with **5** followed by hydrolysis of ester group afforded compound **35**. Displacement of chlorine in **33** using amine **12** and subsequent Suzuki coupling reaction with **5** followed by conversion of nitrile group to tetrazole using NaN_3 gave compound **37** (scheme 3). Suzuki coupling reaction between **5** and **27**–**29** and subsequent reaction with hydrazine hydrate in EtOH followed by cyclization using carbonyldiimidazole gave oxadiazolones **30**–**31** and **38**. *N*-boc group in **30**–**31** was deprotected using TFA/DCM to afford compounds **39** and **40**, respectively.

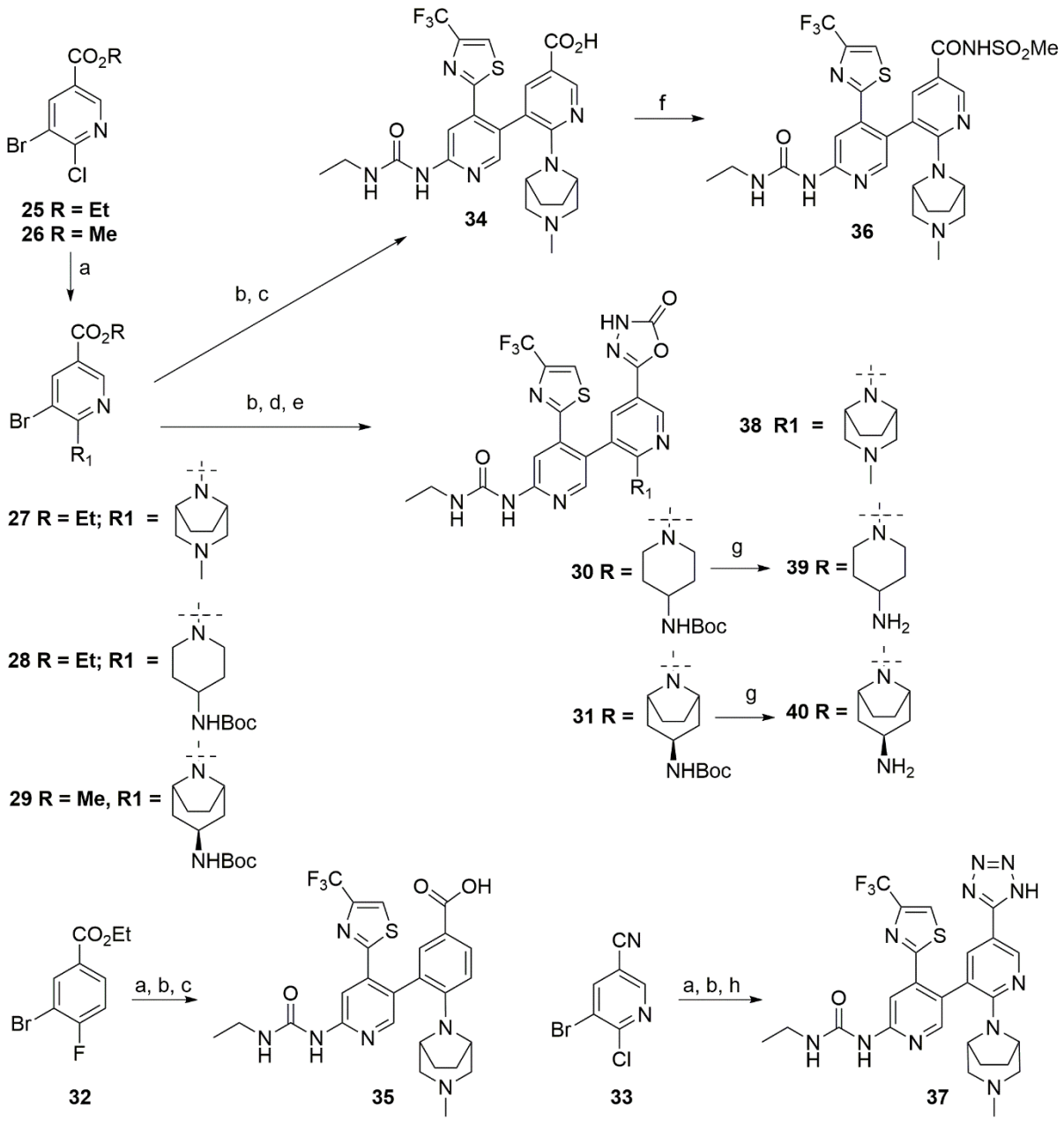

Scheme 3. *Reagents and conditions:* (a) DMF, K_2CO_3, **8**, **9** or **12**, 80 ^oC, 12 h; (b) **5**, K_3PO_4, Pd(dppf)Cl_2.DCM, 1,4-dioxane, water, 100 ^oC, 16 h; (c) LiOH, THF, water; (d) $NH_2NH_2.H_2O$, EtOH, 80 ^oC; (e) CDI, DCM; (f) $MeSO_2NH_2$, HATU, Et_3N, DCM; (g) CF_3CO_2H, CH_2Cl_2, rt, 4 h; (h) NaN_3, $AlCl_3$, DMF, 120 ^oC.

Scheme 4 describes synthesis of compound **44**. Previously reported thioamide **41** [27] was converted to thiazole derivative **43** by heating with **42** in acetonitrile. Conversion of **43** to the corresponding boronic acid, Suzuki coupling with **27**, conversion of the resulting product to

corresponding hydrazide derivative by reaction with hydrazine hydrate and subsequent cyclisation of hydrazide using carbonyldiimidazole resulted in the formation of **44**.

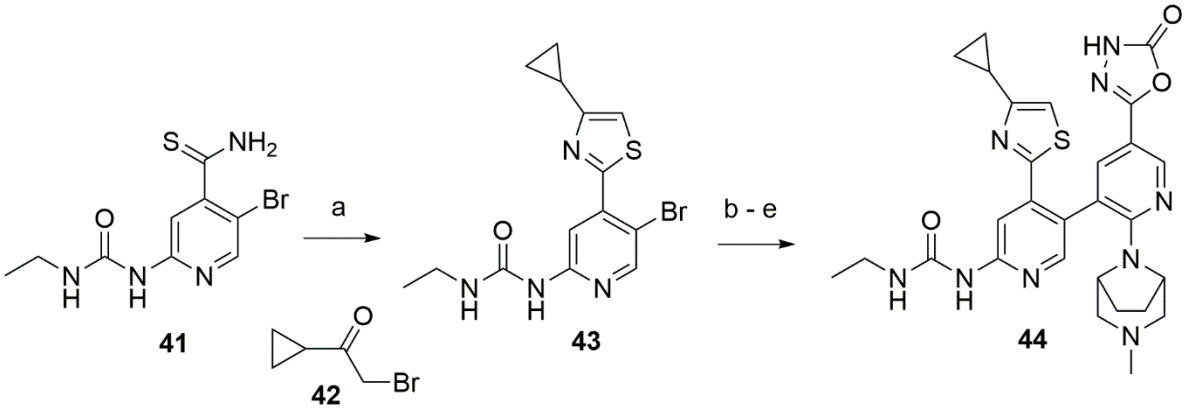

Scheme 4. *Reagents and conditions:* (a) **42**, MeCN, 85 ^{o}C, 16 h; (b) ^{i}PrMgCl, n-BuLi, $B(OMe)_3$, THF, -78 ^{o}C, 6 h; (c) **27**, K_3PO_4, $Pd(dppf)Cl_2$.DCM, 1,4-dioxane, water, 100 ^{o}C, 16 h; (d) $NH_2NH_2.H_2O$, EtOH, 80 ^{o}C; (e) CDI, DIPEA, DCM, rt, 2h.

3. Results and Discussion:

Our chemical starting point **2** exhibited potent inhibition of Gram-positive enzymes *Streptococcus pneumoniae* ParE and *Staphylococcus aureus* GyrB. As mentioned before **2** also potently inhibited a Gram-negative GyrB enzyme (*E.coli*), but was 100-fold less active against ParE from the same bacteria. It did not show an MIC against either wild type or efflux pump impaired *E.coli*. At this point we attributed this result to poor permeability of the compound across bacterial membrane, owing to the presence of a strong acid (pK_a 3.5). Initial exploration of the SAR provided some insight on the key interactions of the compound. Incorporation of a naphthyridine motif in place of pyridine-3-carboxylic acid as in compound **6** (Table 1) not only retained both GyrB and ParE inhibition, but also showed 0.4 µg/mL MIC against *E.coli* ΔtolC strain.

Table 1: IC_{50} (*E.coli* GyrB and *E.coli* ParE) and MIC (*E.coli, P.aeruginosa* and their efflux pump mutants) of **2** and **6**.

		IC_{50} (μM)*		MIC (μg/mL)			
	Structure	E.co GyrB	E.co ParE	P.ae	P.ae ΔMexABCDXY	E.co	E.co ΔtolC
2	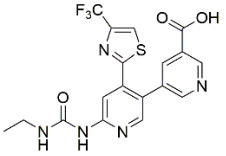	0.006	0.70	>100	>100	>100	>100
6	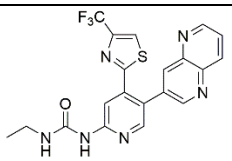	0.004	2.01	>25	>25	>25	0.44

*Standard Error can be found in the supporting information. *E.co* = *E.coli*; *P.ae* = *P.aeruginosa PAO1*; P.ae ΔMexABCDXY = *P.aeruginosa* efflux pump mutant; *E.co ΔtolC* = *E.coli* efflux pump mutant.

The optimization of tricyclic inhibitor **1** involved introduction of the amine to secure an interaction with Asn41 (*Francisella turanrensis* ParE) [18] and suggested that the introduction of an amino group into **6** may be beneficial. In addition, the introduction of the positively charged substituent may improve the permeation of compound across Gram-negative membranes [26, 28].

3.1. Enhancing E.coli ParE inhibition:

We envisaged that introduction of an amino moiety onto the naphthyridine motif might secure an interaction with Asp54 (*S.pneumoniae* ParE) [29, 30]. Compound **14** with a piperazine moiety lead to a 5-fold improvement in ParE inhibition (Table 2). Encouraged by this, we explored various amine substituents at this position. Compound **15** with a 3,6-diazabicyclo[3.1.1]heptane substituent exhibited 10-fold better ParE IC_{50} in comparison to **6.** Compound **16** carrying a 3,8-diazabicyclo[3.2.1]octane motif produced even better ParE inhibition of 14 nM. Attempts to obtain a crystal structure of **16** with *S. pneumoniae* ParE protein were not successful due to the low solubility of the compound. Other bicyclic amines as in compounds **22**, **23** and **24** maintained good inhibitory profile against ParE in the range of ~20 nM. Compound **21** with a 4-aminopiperidine motif also showed ~50 nM IC_{50} against

E.coli ParE. It may be noted that these modifications did not affect IC_{50} values against GyrB enzyme, thus producing better dual inhibition.

Table 2: IC_{50} (*E.coli* GyrB and *E.coli* ParE), MIC (*E.coli*, *P.aeruginosa* and their efflux pump mutants) and pK_a of **6**, **14-16** and **21-24**.

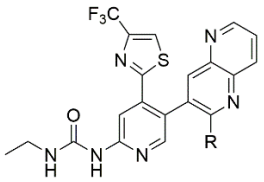

		IC_{50} (µM)*		MIC (µg/mL)				
ID	R	*E.co* GyrB	*E.co* ParE	*P.ae*	*P.ae* ΔMexABCDXY	*E.co*	*E.co* ΔtolC	pK_a
6	-H	0.004	2.011	>25	>25	>25	0.44	ND
14	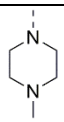	0.003	0.40	>100	1.08	16.82	1.08	7.4
15	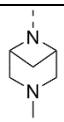	0.005	0.20	>60	1.10	17.19	2.21	7.6
16	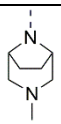	0.007	0.014	9.09	0.56	2.27	0.14	7.8
21	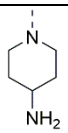	0.006	0.049	67.82	0.54	16.80	0.54	9.3
22	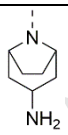	0.003	0.024	35.53	0.56	4.54	0.56	9.2
23	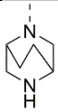	0.008	0.021	>60	0.55	8.87	1.10	9.2
24	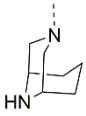	0.014	0.025	>60	0.55	9.09	0.28	9.2

*Standard Error can be found in the supplementary information. *E.co = E.coli*; *P.ae = P.aeruginosa PAO1*; *P.ae ΔMexABCDXY = P.aeruginosa* efflux pump mutant; *E.co* ΔtolC= *E.coli* efflux pump mutant.

As solubility of the scaffold was a limiting factor with the pyridylurea scaffold bearing a naphthyridine moiety, we turned back to compound **2** and decided to introduce the 3,8-diazabicyclo[3.2.1]octane motif (Table 3). Compound **34** exhibited 100-fold improvement in ParE inhibition when compared to **2**. Removal of the pyridyl nitrogen (compound **35**) maintained the inhibitory potency against both targets. Replacing the acid in compound **2** with other acidic functional groups such as methylsulfonamide (**36**) and tetrazole (**37**) derivatives also provided potent inhibitors of *E.coli* ParE. While compound **38** with the oxadiazolone motif in place of the carboxylic acid group exhibited excellent ParE inhibition, compounds **39** and **40** which combine the oxadiazolone with a base containing primary amines gave 6- and 3-fold weaker inhibitors of *E.coli* ParE, respectively. **44** with a cyclopropyl group instead of $-CF_3$ was the most potent compound in this series, exhibiting 3 nM IC_{50} against *E.coli* ParE.

Table 3: IC_{50} (*E.coli* GyrB and *E.coli* ParE), MIC (*E.coli*, *P.aeruginosa* and their efflux pump mutants) and pK_a of **2**, **34**-**40** and **44**.

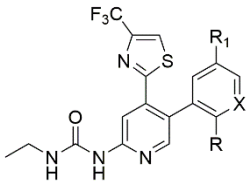

ID	R	R1	X	IC_{50} (μM)*		MIC (μg/mL)				pK_a
				E.co GyrB	*E.co* ParE	*P.ae*	*P.ae* ΔMexABCDXY	*E.co*	*E.co* ΔtolC	
2	H	-COOH	N	0.006	0.70	>100	>100	>100	>100	3.5
34	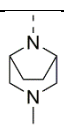	-COOH	N	0.006	0.008	9.0	4.48	9.0	1.12	3.5, 7.4
35		-COOH	C	0.009	0.01	9.0	4.46	9.0	1.12	4.4, 8.2

36		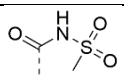	N	0.008	0.009	>50	>50	>50	>50	3.2, 7.6
37			N	0.009	0.004	>50	>50	>50	36	3.6, 7.8
38		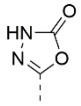	N	0.006	0.004	2.40	0.30	1.20	0.12	6.7, 7.8
39	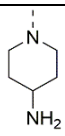	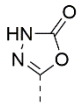	N	0.002	0.023	>50	1.15	>50	9.20	6.8, 9.5
40			N	0.004	0.012	>50	0.60	>50	4.80	6.8, 9.5
44	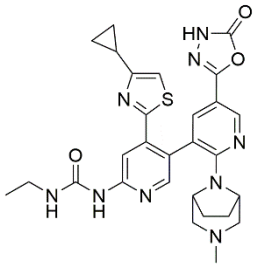			0.002	0.003	1.14	0.23	0.57	0.11	6.7, 7.9

*Standard Error can be found in the supplementary information. *E.co = E.coli*; *P.ae = P.aeruginosa PAO1*; *P.ae ΔMexABCDXY = P.aeruginosa* efflux pump mutant; *E.co* ΔtolC= *E.coli* efflux pump mutant.

Compound **38** was co-crystallized with *S. pneumoniae* ParE (fig. 2, PDB ID 5YIG). The nitrogen from the 3,8-diazabicyclo[3.2.1]octane motif interacts with Asp54 (corresponding residue in *E.coli* ParE is Asp45), confirming our expectation. The X-ray crystal structure also shows the ethylene bridge of bicyclic amine nicely fitting into the small pocket between Arg81 and Asp54, further explaining the preference for such bicyclic groups and the improvement in ParE inhibition. The pyridine ring and the oxadiazolone motif ensure good interactions with Arg81 and Arg140, respectively. The rest of the interactions were as observed earlier for the scaffold [27].

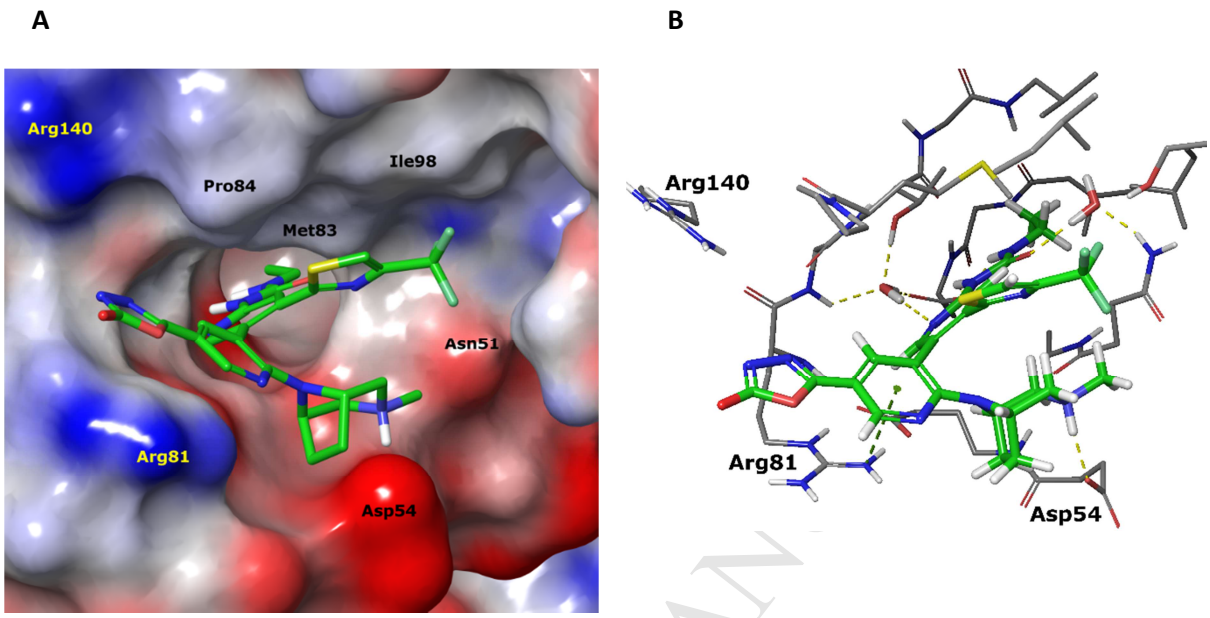

Fig. 2: (A) Crystal structure of **38** with *S. pneumoniae* ParE (PDB ID 5YIG). The nitrogen from the 3,8-diazabicyclo[3.2.1]octane motif interacts with Asp54 (shown with dotted lines in B).

3.2. The influence of dual target inhibition and pK_a of the amines on MIC

For a potent dual GyrB/ParE inhibitor to show an MIC against Gram-negative bacteria, the compound has to permeate through the Gram-negative membrane to reach the cytoplasm and then avoid being removed by the efflux pumps. Thus, in order to evaluate the effect of improved target inhibition and/or compound permeability on the growth of bacteria, we compared the MIC of *P.aeruginosa* and *E.coli* wild type with bacteria that have deletions of multidrug resistance pumps.

Most compounds in Table 2 were moderate inhibitors of wt *E.coli* but showed no activity against wt *P.aeruginosa*. Compound **16** was most potent exhibiting 9 and 2.2 µg/mL MIC

against *P.aeruginosa* and *E.coli*, respectively. From these data we have to conclude that dual target inhibition alone does not necessarily result in good MICs against these two pathogens.

Looking more closely at the compounds in Table 2 we can observe two major effects on the MICs (keeping in mind that all compounds are very potent inhibitors of the *E.coli* GyrB enzyme). First, if the basic pK_a value of the inhibitors are comparable then greater ParE enzyme inhibition leads to a better MIC (compare **15** and **16** in Table 2). Second, when we have dual inhibitors with potent inhibition of ParE, then the pK_a of the amine has a major effect on the efflux of the compounds, as can be seen when comparing compound **16** with **21**–**24**. The effect of the pK_a on efflux seems to be more pronounced on *P.aeruginosa*, while the effect of dual target inhibition is more pronounced on *E. coli*. When the pK_a of the conjugate acid of the amine was greater than 9, their MIC against wt *P.aeruginosa* were >30 µg/mL, suggesting that these compounds suffer enhanced efflux in wt *P.aeruginosa* (compare with the corresponding efflux mutants in Table 2). Among the compounds with identical target inhibition (**16**, **21**–**24**), **16** with pK_a 7.8 showed improved MICs against both wt *P.aeruginosa* and *E. coli* species. The weaker MICs exhibited by **14** and **15** (despite their pK_a of ~7.5) may be due to its lack of dual target inhibition.

3.3. The influence of the pK_a of the acids on MIC

While a basic amine aids compound permeability across Gram-negative membranes, the presence of a carboxylic group is not favorable for the pyridylurea scaffold, as indicated by the MIC of compound **2** in Table 3 which is >100 µg/mL against both wt and efflux mutant forms of both Gram-negative species tested. When introducing 3-methyl-3,8-diazabicyclo[3.2.1]octane as the most favorable basic group from Table 2, the permeability of compound **2** is improved considerably (see compound **34** in Table 3). Compounds **36** and **37** carrying a sulfonamide and tetrazole moiety in place of carboxylic acid group did not show an MIC against even the efflux mutant of *P.aeruginosa* and *E.coli*. In contrast,

compound **38** with a 1,3,4-oxadiazol-2(3H)-one motif showed significant improvement with an MIC value of 2.4 and 1.2 µg/mL against wt *P.aeruginosa* and *E.coli*. Again compounds **39** and **40** with a primary amine as basic moiety (pK_a = 9.5) showed >50 µg/mL MIC against wt *P.aeruginosa* and *E.coli*. Compound **44** which has the best combination of dual inhibition, basic and acidic pK_a proved to have the best MIC of 1 and 0.5 µg/mL against the two pathogens. It is clear from the compounds in Table 3 that a weaker acidic moiety such as 1,3,4-oxadiazol-2(3H)-one motif in **38** with a pK_a of 6.8 is preferred for better MIC. Compounds **39** and **40** again show that the presence of a more basic amine leads to enhanced efflux in *P.aeruginosa*. Thus the combination of a weak acid and a weak base provide the best MIC for pyridylurea GyrB/ParE dual inhibitors.

3.4. Broad-Spectrum Activity

We tested compounds **16**, **38** and **44** for their broad-spectrum activity (Table 4). Potent growth inhibition was observed against *A. baumannii* and *Haemophilus influenzae*. Against *A. baumannii*, **16**, **38** and **44** exhibited MICs of 2, 0.5 and 0.5 µg/mL, respectively. The compounds were also active against several Gram-positive pathogens, including fluoroquinolone resistant MRSA and USA 100 MRSA with <0.06 µg/mL MICs, illustrating broad spectrum activity. These compounds showed higher MICs against *Klebsiella pneumoniae* and *Enterobacter cloacae*. Gratifyingly, no activity was seen at the highest concentration tested against the fungal pathogen *Candida albicans*, indicating selectivity for prokaryotes.

Table 4: MIC (µg/mL) against other Gram-negative and Gram-positive species

Species	Linezolid	Ceftazidime	**16**	**38**	**44**
A. baumannii[a]	>64	>32	2	0.5	0.5
H. influenzae[b]	4	0.25	0.25	<0.06	<0.06
E.cloacae[c]	>64	>32	>64	32	16

K.pneumoniae[d]	>64	0.25	64	32	16
S.aureus[e]	2	16	<0.06	<0.06	<0.06
S.aureus[f]	2	16	<0.06	<0.06	<0.06
S.aureus[g]	0.5	>32	<0.06	<0.06	<0.06
S.aureus[h]	1	>32	<0.06	<0.06	<0.06
S.pyogenes[i]	0.5	0.125	<0.06	<0.06	<0.06
S.pneumoniae[j]	1	0.5	<0.06	<0.06	<0.06
E.faecalis[k]	1	>32	<0.06	<0.06	<0.06
C.albicans[l]	>64	>32	>64	>64	>64

[a]*Acinetobactor baumannii* ARC3495; [b] *Haemophilus influenzae* ATCC49247; [c]*Enterobacter cloacae* ARC3528; [d]*Klebsiella pneumoniae* ARC1865; [e]*Staphylococcus aureus* ATCC29213; [f]ATCC29213 + 2% Human albumin; [g]MRSA FQ-R; [h]USA100 MRSA; [i]*Streptococcus pyogenes ARC838;* [j]*Streptococcus pneumoniae* ATCC 49619; [k]*Enterococcus faecalis* ATCC 29212; [l]*Candida albicans* ATCC 90028.

Population MIC of compounds against 20 strains [31, 32] of *P.aeruginosa* and *A.baumannii* showed **44** as the most potent compound with MIC_{90}'s of 4 and 2 µg/mL, respectively. **38** showed 8 and 4 µg/mL MIC_{90} against *P.aeruginosa* and *A.baumannii* while **16** showed 32 and 4 µg/mL, respectively (Table 5).

Table 5: MIC_{90} (µg/mL) against *P.aeruginosa* and *A.baumannii* (n = 20*):

	*P. aeruginosa**	*A. baumannii**
Meropenem	>64	>64
16	32	4
38	8	4
44	4	2

*20 strains were used.

Compound **38** was further tested for its properties. It showed thermodynamic solubility of 1490 µM at pH 7.4. **38** also showed lower protein binding compared to **16** and **44** (Table 6).

Table 6: Solubility and Plasma Protein Binding of **16**, **38** and **44**

	16	**38**	**44**
Thermodynamic Solubility (µM)	Below detection limit	1490	65.8
PPB human (%)	97.0	78.9	85.1

4. Conclusions

The dearth of new drugs for the treatment of Gram-negative infections is mainly due to difficulties of achieving acceptable MICs for target based inhibitors. There have been publications [26, 28] that tried to describe the physical properties required for small molecule accumulation in Gram-negative bacteria. O'Shea and Moser [26] found that antibiotics with Gram-negative activity seem to be relatively polar (average cLogD7.4 of -2.8), have a relatively high molecular weight (< 600 g/mol) and are sometimes zwitterionic, while Richter *et al.*[28] suggested that an amine functional group and properties like amphiphilicity, globularity and rigidity influence the accumulation of compounds in Gram-negative bacteria. Such predictive compound accumulation rules can be useful, however in the case of target-based drug discovery they must be combined with the functional groups required for molecular recognition. Our data clearly shows the importance of dual target inhibition (GyrB and ParE) and optimal permeability which can be achieved with the introduction of a basic amine at the appropriate position. A zwitterionic compound is beneficial in our case, because it ensures that the compounds have appropriate solubility, however tuning of the pK_a of both the acid and the base is essential for an optimal MIC.

5. Experimental Section:

5.1. General Procedures. All reagents were purchased from commercial sources and used as received. Reaction progress was monitored by TLC using Merck silica gel 60 F254 on glass

plates with detection by UV at 254 nM. LC−MS analysis was carried out with a Shimadzu LC-20AD and LCMS-2020. The column used was a Phenomenex Kinetex 2.6 μm, 50 × 2.10 mm). HRMS was obtained from a Thermo Scientific Orbitrap Fusion mass spectrometer coupled with Advion TriVersa NanoMate (detector Orbitrap high resolution, resolution 120000, mass accuracy <5 ppm). Proton nuclear magnetic resonance (^{1}H NMR) spectra were obtained using a Bruker Ultrashield 400 PLUS/R system, operating at 400 MHz. All resonance bands were referenced to tetramethylsilane (internal standard). Splitting patterns are indicated as follows: s, singlet; d, doublet; t, triplet; m, multiplet; br, broad peak. The compounds' purities were ≥95% unless otherwise stated, determined by a VARIAN ProStar HPLC instrument. Melting points (mp) were determined in Pyrex capillary tubes using a StuartnSMP30 melting point apparatus. Purification of final compounds and intermediates was carried out via normal or reverse phase chromatography. Normal-phase chromatography was performed on an ISCO CombiFlash system with either an ISCO RediSep or a Biotage silica gel disposable column eluted with EtOAc/hexanes or MeOH/CH_2Cl_2. Reverse-phase chromatography was performed on a Shimadzu preparative system on a Phenomenex Luna or Sunfire C18 preparative column with appropriate gradients of MeCN/H_2O/0.1% trifluoroacetic acid (TFA) or methanol/H_2O/0.1% TFA as eluent at a flow rate of 40 mL/min.

5.1.1. General procedure for Suzuki coupling reaction: To a solution of aryl bromide (0.3 mmol) in anhydrous 1,4-dioxane (10 mL) was added boronic acid (0.45 mmol) and a solution of K_3PO_4 (130 mg, 0.61 mmol) in water (2 mL). The mixture was purged with nitrogen gas for 5 minutes. Pd(dppf)Cl_2.CH_2Cl_2 (12 mg, 0.015 mmol) was added and the mixture was heated at 100 ^oC. After 5 h, the reaction mixture was cooled to room temperature, filtered through celite and washed with ethyl acetate. The filtrate was washed with water (50 mL), brine (50 mL), dried (anhydrous Na_2SO_4) and concentrated under reduced pressure. The

residue was purified by preparative HPLC (C18 column, 20:80 acetonitrile / water with 0.1% formic acid). Compound containing fractions were lyophilized to afford the product.

*5.1.2. 1-(5-(1,5-Naphthyridin-3-yl)-4-(4-(trifluoromethyl)thiazol-2-yl)pyridin-2-yl)-3-ethylurea (**6**):* Synthesized from **4** and **5** following the general procedure for Suzuki coupling in 58 % yield as a pale yellow solid. ^{1}H NMR (400 MHz, DMSO-d_6) δ 9.52 (s, 1H), 9.05−9.04 (m, 1H), 8.82−8.81 (m, 1H), 8.50−8.46 (m, 4H), 8.26 (s, 1H), 7.85−7.82 (m, 1H), 7.62−7.59 (m, 1H), 3.27−3.19 (m, 2H), 1.12 (t, 3H, *J* = 7.2 Hz); ^{13}C NMR (100 MHz, DMSO-d_6) δ 165.7, 153.7, 153.5, 151.6, 151.3, 149.1, 142.8, 142.4, 142.2, 142.0, 141.8, 138.7, 136.4, 136.1, 132.7, 125.7, 125.6, 124.5, 123.6, 120.9, 118.3, 115.6, 109.6, 33.4, 14.7. MS (ESI) *m/z* 445.1 $(M+H)^+$; HRMS: calcd for $C_{20}H_{15}F_3N_6OS$ $(M+H)^+$, 445.1053; found, 445.1046. mp: 232.4−232.7 °C.

*5.1.3. 1-Ethyl-3-(5-(2-(4-methylpiperazin-1-yl)-1,5-naphthyridin-3-yl)-4-(4-(trifluoromethyl)-thiazol-2-yl)pyridin-2-yl)urea (**14**):* To a solution of **7** (150 mg, 0.61 mmol) in DMF (5 mL) was added K_2CO_3 (256.6 mg, 1.8 mmol) and *N*-methyl piperazine (0.3 mL, 3.0 mmol). After heating at 80 ^{o}C for 4 h, the reaction mixture was cooled to room temperature, poured in to cold water (20 mL) and extracted with EtOAc (2 × 50 mL). The combined organic layer was washed with water, brine, dried over Na_2SO_4 and concentrated to afford 3-bromo-2-(4-methylpiperazin-1-yl)-1,5-naphthyridine [150 mg, ^{1}H NMR (400 MHz, DMSO-d_6) δ 8.79-8.76 (m, 1H), 8.59 (s, 1H), 8.16 (d, 1H, *J* = 8.4 Hz), 7.71-7.67 (m, 1H), 3.48-3.41 (m, 4H), 2.90-2.88 (m, 1H), 2.75-2.73 (m, 1H), 2.58-2.52 (m, 2H), 2.26 (s, 3H); MS (ESI) *m/z* 308.8 $(M+H)^+$, 309.8 $(M+2+H)^+$]. This intermediate was subjected to Suzuki coupling with **5** according to the general procedure to afford **14** in 30 % yield as an off-white solid. ^{1}H NMR (400 MHz, DMSO-d_6) δ 9.48 (s, 1H), 8.80 (t, 1H, *J* = 3.0 Hz), 8.51 (s, 1H), 8.38 (s,1H), 8.28 (s,1H), 8.22 (s, 1H), 8.14 (d, 1H, *J* = 8.0 Hz), 7.68 (dd, 2H, *J* = 4.0, 8.8 Hz), 3.26-3.20 (m, 2H), 2.98-2.93 (m, 2H), 2.80-2.72 (m, 2H), 2.14-2.02 (m, 4H), 1.99-1.81 (m, 2H), 1.12 (t,

3H, *J* = 7.2 Hz); ^{13}C NMR (100 MHz, DMSO-d_6) δ 166.3, 157.9, 153.7, 153.3, 148.6, 147.8, 142.5, 142.1, 141.7, 141.5, 141.4, 140.8, 140.2, 139.1, 138.2, 137.4, 133.9, 127.3, 124.5, 124.4, 124.3, 123.8, 121.1, 118.4, 109.3, 52.9, 47.7, 44.7, 33.3, 14.7; MS (ESI) *m/z* 543.1 $(M+H)^+$; HRMS: calcd for $C_{25}H_{25}F_3N_8OS$ $(M+H)^+$, 543.1897; found 543.1896. mp: 242.3 - 244.6 °C.

*5.1.4. 1-Ethyl-3-(5-(2-(3-methyl-3,6-diazabicyclo[3.1.1]heptan-6-yl)-1,5-naphthyridin-3-yl)-4-(4-(trifluoromethyl)thiazol-2-yl)pyridin-2-yl)urea (**15**):* Synthesized in 3 % yield following the procedure described for **14**, using **13** as the amine as an off-white solid. ^{1}H NMR (400 MHz, DMSO-d_6) δ 9.45 (s, 1H), 8.67 (dd, 1H, *J* = 4.0, 1.2 Hz), 8.44 (s, 2H), 8.24 (s, 1H), 8.14 (s, 1H), 8.00 (d, 1H, *J* = 8.0 Hz), 7.62-7.59 (m, 2H), 3.98 (s, 1H), 3.42 (s, 1H), 3.25-3.18 (m, 2H), 3.13 (d, 1H, *J* = 8.8 Hz), 2.58 (d, 1H, *J* = 10.4 Hz), 2.02 (s, 3H), 1.67 (d, 1H, *J* = 7.2 Hz), 1.11 (t, 3H, *J* = 7.2 Hz); ^{13}C NMR (100 MHz, DMSO-d_6) δ 166.3, 155.8, 154.8, 154.5, 149.5, 147.2, 143.6, 143.4, 143.2, 142.8, 142.5, 140.8, 140.6, 140.4, 134.0, 126.6, 125.4, 124.9, 124.6, 124.2, 122.2, 119.5, 109.7, 62.2, 61.4, 54.9, 52.6, 43.1, 34.4, 29.0, 15.8; MS (ESI) *m/z* 555.1 $(M+H)^+$; HRMS: calcd for $C_{26}H_{25}F_3N_8OS$ $(M+H)^+$, 555.1897; found 555.1900. mp: 207.1−207.5 °C.

*5.1.5. 1-Ethyl-3-(5-(2-(3-methyl-3,8-diazabicyclo[3.2.1]octan-8-yl)-1,5-naphthyridin-3-yl)-4-(4-(trifluoromethyl)thiazol-2-yl)pyridin-2-yl)urea (**16**):* Synthesized in 16 % yield following the procedure described for **14**, using **12** as the amine as an off-white solid. ^{1}H NMR (400 MHz, DMSO-d_6) δ 9.48 (s, 1H), 8.73 (d, 1H, *J* = 3.2 Hz), 8.48 (s, 1H), 8.41 (s, 1H), 8.22 (d, 1H, *J* = 7.2 Hz), 8.05 (d, 1H, *J* = 8.4 Hz), 7.70 (s, 1H), 7.66-7.62 (m, 1H), 4.04 (d, 1H, *J* = 6.4 Hz), 3.64 (d, 1H, *J* = 6.8 Hz), 3.25-3.17 (m, 2H), 2.39 (d, 1H, *J* = 10 Hz), 2.27 (d, 1H, *J* = 8.4 Hz), 2.03 (d, 1H, *J* = 10 Hz), 1.99 (s, 3H), 1.83-1.75 (m, 1H), 1.69-1.57 (m, 2H), 1.44 (d, 1H, *J* = 10 Hz), 1.34-1.32 (m, 1H), 1.12 (t, 3H, *J* = 7.2 Hz); ^{13}C NMR (100 MHz, DMSO-d_6) δ 166.9, 156.6, 154.8, 154.3, 149.5, 148.1, 143.5, 143.1, 142.8, 142.7, 142.4, 141.5,

141.4, 139.4, 134.6, 127.1, 125.9, 125.7, 125.4, 124.9, 122.2, 119.5, 110.2, 60.3, 58.8, 58.6, 55.7, 44.5, 34.4, 28.3, 26.9, 15.8; MS (ESI) *m/z* 569.2 $(M+H)^+$; HRMS: calcd for $C_{27}H_{27}F_3N_8OS$ $(M+H)^+$, 569.2053; found 569.2053. mp: 219.0-219.9 °C.

*5.1.6. 1-(5-(2-(4-Aminopiperidin-1-yl)-1,5-naphthyridin-3-yl)-4-(4-(trifluoromethyl)thiazol-2-yl)pyridin-2-yl)-3-ethylurea (**21**):* A mixture of **7** (122 mg, 0.50 mmol), **8** (300 mg, 1.5 mmol) and K_2CO_3 (207 mg, 1.5 mmol) in DMF (4 mL) was heated at 80 ^oC. After 3 h, the reaction mixture was diluted with water and extracted with EtOAc (2 x 50 mL). Organic layer was washed with brine, dried (Na_2SO_4) and evaporated. The residue (200 mg crude) was subjected to Suzuki coupling condition as mentioned in the general procedure with **5** to afford **17** (30 mg) which was subsequently treated with TFA in 3 mL DCM. After 4 h, the reaction mixture was diluted with DCM, washed with sat. aq. $NaHCO_3$, brine, dried (Na_2SO_4) and evaporated. The residue was re-dissolved in 1 mL DCM and triturated with hexane. The solid formed was filtered to afford **21** (18 mg, 9 % yield) as a white solid. ^{1}H NMR (400 MHz, DMSO-d_6) δ 9.49 (s, 1H), 8.77 (d, 1H, *J* = 3.2 Hz), 8.51 (s, 1H), 8.40 (s, 1H), 8.25 (s, 1H), 8.21 (s, 1H), 8.11 (d, 1H, *J* = 8.4 Hz), 7.67-7.64 (m, 2H), 3.25-3.16 (m, 4H), 3.08 (d, 1H, *J* = 12 Hz), 2.72 (d, 1H, *J* = 12 Hz), 2.38 (d, 1H, *J* = 12 Hz), 1.49 (d, 1H, *J* = 11.6 Hz), 1.33 (d, 1H, *J* = 9.2 Hz), 1.12 (t, 3H, *J* = 7.2 Hz), 0.98-0.85 (m, 1H), 0.64-0.62 (m, 1H); ^{13}C NMR (100 MHz, DMSO-d_6) δ 167.4, 159.7, 154.8, 154.3, 149.6, 148.7, 143.2, 142.8, 142.5, 141.8, 141.0, 139.2, 134.9, 128.7, 125.6, 125.5, 125.3, 124.8, 122.1, 119.5, 110.4, 48.6, 48.2, 47.2, 34.8, 34.6, 34.4, 15.8; MS (ESI) *m/z* 543.2 $(M+H)^+$; mp: 249.1−250.9 °C.

*5.1.7. 1-(5-(2-((1R,3r,5S)-3-amino-8-azabicyclo[3.2.1]octan-8-yl)-1,5-naphthyridin-3-yl)-4-(4-(trifluoromethyl)thiazol-2-yl)pyridin-2-yl)-3-ethylurea (**22**):* Synthesized in 12% yield as described in the procedure for **21** using **9** as the amine (off-white solid). ^{1}H NMR (400 MHz, DMSO-d_6) δ 9.43 (s, 1H), 8.70 (s, 1H), 8.47 (s, 1H), 8.40 (s, 1H), 8.23 (s, 1H), 8.15 (s, 1H),

8.03 (d, 1H, *J* = 7.6 Hz), 7.63 (s, 2H), 3.90 (s, 1H), 3.24-3.20 (m, 2H), 2.87-2.84 (m, 1H), 1.76-1.74 (m, 1H), 1.47-1.24 (m, 6H), 1.14-1.12 (m, 3H); MS (ESI) *m/z* 569.2 $(M+H)^+$.

*5.1.8. 1-(5-(2-(2,5-Diazabicyclo[2.2.2]octan-2-yl)-1,5-naphthyridin-3-yl)-4-(4-(trifluoro-methyl)thiazol-2-yl)pyridin-2-yl)-3-ethylurea (**23**):* Synthesized as described in the procedure for **21** in 5% yield as a white solid. ^{1}H NMR (400 MHz, DMSO-d_6) δ 9.50 (s, 1H), 8.72 (s, 1H), 8.52 (d, 1H, *J* = 13.6 Hz), 8.45 (d, 1H, *J* = 12.4 Hz), 8.24-8.19 (m, 2H), 8.06-8.03 (m, 1H), 7.66-7.63 (m, 2H), 4.16-3.86 (m, 1H), 3.43 (d, 1H, *J* = 13.6 Hz), 3.23-3.12 (m, 4H), 3.03 (d, 1H, *J* = 11.2 Hz), 2.87-2.79 (m, 1H), 2.69-2.66 (m, 1H), 1.79-1.77 (m, 1H), 1.70-1.38 (m, 2H), 1.27-1.23 (m, 1H), 1.15 (t, 3H, *J* = 7.2 Hz); MS (ESI) *m/z* 555.2 $(M+H)^+$; mp: 226.2−227.1 °C.

*5.1.9. 1-(5-(2-(3,9-diazabicyclo[3.3.1]nonan-3-yl)-1,5-naphthyridin-3-yl)-4-(4-(trifluoro-methyl)thiazol-2-yl)pyridin-2-yl)-3-ethylurea (**24**):* Synthesized as described in the procedure for **21** in 4% yield. ^{1}H NMR (400 MHz, DMSO-d_6) δ 9.50 (s, 1H), 8.79 (d, 1H, *J* = 2.8 Hz), 8.49 (s, 1H), 8.45 (s, 1H), 8.40 (s, 1H), 8.18 (s, 1H), 8.16 (s, 1H), 7.72-7.69 (m, 1H), 7.55 (s, 1H), 3.80 (d, 1H, *J* = 13.2 Hz), 3.49-3.42 (m, 3H), 3.23-3.16 (m, 3H), 3.05 (d, 1H, *J* = 13.2 Hz), 1.80 (br s, 3H), 1.47 (d, 1H, *J* = 9.2 Hz), 1.30 (d, 1H, *J* = 8.4 Hz), 1.23 (s, 1H), 1.11 (t, 3H, *J* = 7.2 Hz); MS (ESI) *m/z* 569.2 $(M+H)^+$.

*5.1.10. Ethyl 5-bromo-6-(3-methyl-3,8-diazabicyclo[3.2.1]octan-8-yl)nicotinate (**27**):* To a well stirred solution of **25** (8.6 g, 32.8 mmol) in DMF (50 mL) were added **12** (9.7 g, 49.0 mmol) and K_2CO_3 (8.8 g, 64.0 mmol). After heating at 80 °C for 4 h, the reaction mixture was cooled, diluted with water (50 mL) and extracted with EtOAc (3 x 60 mL). The combined organic layer was washed with brine, dried over Na_2SO_4 and evaporated. The residue was purified by column chromatography (silica gel, eluent EtOAc/ hexane 2:7) to afford **27** (6.0 g, 97 % yield). ^{1}H NMR (400 MHz, $CDCl_3$) δ 8.71 (d, 1H, *J* = 2.0 Hz), 8.27 (d,

1H, *J* = 2.0 Hz), 4.79 (s, 2H), 4.35 (q, 2H, *J* = 7.2 Hz), 2.73 (d, 2H, *J* = 11.2 Hz), 2.43 (d, 2H, *J* = 10.8 Hz), 2.26 (s, 3H), 1.99–1.85 (m, 4H), 1.36 (t, 3H, *J* = 7.2 Hz); MS (ESI) *m/z* 354.4 $(M+H)^+$, 356.3 $(M+2+H)^+$.

*5.1.11. Ethyl 5-bromo-6-(4-((tert-butoxycarbonyl)amino)piperidin-1-yl)nicotinate (**28**):* Synthesized from **25** using **8** as the amine in 68 % yield. ^{1}H NMR (400 MHz, DMSO-d_6) δ 8.68 (d, 1H, *J* = 2.0 Hz), 8.23 (d, 1H, *J* = 2.0 Hz), 6.91 (d, 1H, *J* = 8.4 Hz), 4.31-4.26 (m, 2H), 3.94 (d, 2H, *J* = 13.2 Hz), 3.49 (d, 1H, *J* = 7.2 Hz), 2.96 (t, 2H, *J* = 11.2 Hz), 1.83 (d, 2H, *J* = 10.4 Hz), 1.55–1.45 (m, 2H), 1.39 (s, 9H), 1.30 (t, 3H, *J* = 7.2 Hz); MS (ESI) *m/z* 428.09 $(M+H)^+$, 430.09 $(M+2+H)^+$.

*5.1.12. Methyl 5-bromo-6-((1R,3r,5S)-3-((tert-butoxycarbonyl)amino)-8-azabicyclo[3.2.1]octan-8-yl)-nicotinate (**29**):* Synthesized from **26** using **9** as amine in 80% yield. MS (ESI) *m/z* 440.1 $(M+H)^+$, 442.1 $(M+2+H)^+$.

*5.1.13. 6'-(3-Ethylureido)-2-(3-methyl-3,8-diazabicyclo[3.2.1]octan-8-yl)-4'-(4-(trifluoro-methyl)thiazol-2-yl)-[3,3'-bipyridine]-5-carboxylic acid (**34**):* Suzuki coupling between **27** (50.0 mg, 0.14 mmol) and **5** (79.39 mg, 0.22 mmol) was carried out as per the general procedure. The product [34.2 mg, MS (ESI) *m/z* 576.2 $(M+H)^+$] was dissolved in THF (3 mL) and water (1 mL) and treated with LiOH (13.73 mg, 0.57 mmol). After 3 h, the reaction mixture as evaporated and the residue purified by preparative HPLC (C18, gradient elution using MeCN and water containing formic acid 0.1%). The product containing fractions were lyophilized to afford **34** (20.8 mg, 64 % yield over two steps). ^{1}H NMR (400 MHz, DMSO-d_6) δ 9.43 (s, 1H), 8.73 (d, 1H, *J* =2.0 Hz), 8.48 (s, 1H), 8.35 (s, 1H), 8.21 (s, 1H), 7.91 (d, 1H, *J* =2.4 Hz), 7.64 (s, 1H), 3.94 (s, 1H), 3.82-3.81 (m, 1H), 3.22-3.19 (m, 2H), 2.36-2.28 (m, 2H), 1.96 (s, 4H), 1.62-1.50 (m, 4H), 1.32-1.30 (m, 1H), 1.11 (t, 3H, *J* =7.2 Hz); ^{13}C NMR (100 MHz, DMSO-d_6) δ 166.2, 165.9, 163.0, 158.3, 154.3, 153.7, 150.2, 148.8, 142.7,

142.3, 141.8, 138.8, 125.6, 125.5, 121.8, 119.1, 117.8, 117.5, 109.5, 59.6, 58.3, 56.8, 54.8, 44.4, 33.9, 27.5, 26.6, 15.3; MS (ESI) *m/z* 562.2 $(M+H)^+$; HRMS: calcd for $C_{25}H_{26}F_3N_7O_3S$ $(M+H)^+$, 562.1843; found 562.1843. mp: 233.0−236.6 °C.

*5.1.14. 3-(6-(3-Ethylureido)-4-(4-(trifluoromethyl)thiazol-2-yl)pyridin-3-yl)-4-(3-methyl-3,8-diazabicyclo[3.2.1]octan-8-yl)benzoic acid (**35**):* **32** (300 mg, 1.2 mmol) in anhydrous DMF (4 mL) was treated with **18** (dihydrochloride salt, 483 mg, 2.4 mmol) and K_2CO_3 (671 mg, 4.8 mmol). After 20 h at 100 °C, the reaction mixture was cooled to room temperature and partitioned between water (40 mL) and EtOAc (40 mL). The organic layer was washed with brine (50 mL), dried (anh. sodium sulfate), concentrated and the residue purified by flash chromatography (Redisep silica gel, 0−100% hexanes/ethyl acetate) to afford ethyl 3-bromo-4-(3-methyl-3,8-diazabicyclo[3.2.1]octan-8-yl)benzoate [74 mg, MS (ESI) *m/z* 353.0 $(M+H)^+$, 355.0 $(M+2+H)^+$]. Suzuki coupling between this compound (74 mg, 0.2 mmol) and **5** (112 mg, 0.31 mmol) was carried out as described in the general procedure. The crude product [38 mg, MS (ESI) *m/z* 589.2 $(M+H)^+$] was dissolved in 4 mL of THF and water (1:1) containing LiOH (28 mg, 1.2mmol). After 16 h at 80 °C, the reaction mixture was concentrated and the residue purified by reversed phase preparative HPLC (7:3 water:MeCN containing 0.1% formic acid). Fractions containing the product were combined and lyophilized to afford **35** (19.2 mg, 3 % over three steps). ^{1}H NMR (400 MHz, DMSO-d_6) δ 9.38 (s, 1H), 8.41 (s, 1H), 8.29 (s, 1H), 8.20 (s, 1H), 7.91−7.88 (m, 1H), 7.75−7.73 (m, 2H), 6.97 (d, 1H, *J* = 8.6 Hz), 3.51 (br s, 2H), 3.42−3.40 (m, 2H), 3.25−3.18 (m, 3H), 2.32−2.30 (m, 1H), 2.25−2.23 (m, 1H), 1.88−1.84 (m, 1H), 1.75−1.66 (m, 2H), 1.61−1.57 (m, 1H), 1.42−1.39 (m, 1H), 1.25 (s, 1H), 1.12 (t, 3H, *J* = 7.2 Hz); ^{13}C NMR (100 MHz, DMSO-d_6) δ 166.4, 165.8, 153.8, 152.7, 151.4, 148.2, 141.6, 141.3, 138.5, 133.6, 131.1, 126.7, 125.3, 124.7, 122.5, 121.3, 118.6, 116.6, 108.9, 59.2, 58.6, 57.8, 55.8, 43.9, 33.3, 26.9, 25.9, 14.7. MS (ESI) *m/z* 561.1 $(M+H)^+$; mp: 232.5−233.0 °C.

*5.1.15. 6'-(3-Ethylureido)-2-(3-methyl-3,8-diazabicyclo[3.2.1]octan-8-yl)-N-(methylsulfonyl)-4'-(4-(trifluoromethyl)thiazol-2-yl)-[3,3'-bipyridine]-5-carboxamide (**36**):* **34** (100 mg, 0.18 mmol) in anhydrous DMF (3 mL) was treated with HATU (102 mg, 0.0.27 mmol), methanesulfonamide (22 mg, 0.24 mmol) and anhydrous Et_3N (0.06 mL, 0.4 mmol). After 2 h at room temperature, the reaction mixture was partitioned between water and EtOAc. The organic layer was washed with brine, dried (Na_2SO_4) and evaporated. The residue was purified by preparative HPLC (7:3 water:MeCN containing 0.1% formic acid). Product containing fractions were lyophilized to afford **36** (38 mg, 22% yield over 2 steps). ^{1}H NMR (400 MHz, CD_3OD) δ 8.88 (s, 1H), 8.39 (s, 1H), 8.21−8.17 (m, 2H), 7.88 (s, 1H), 4.06−4.04 (m, 1H), 3.90−3.89 (m, 1H), 3.38−3.34 (m, 4H), 3.13 (s, 3H), 3.01 (br s, 2H), 2.56 (s, 3H), 2.32 (s, 1H), 2.06−2.05 (m, 1H), 1.76−1.65 (m, 2H), 1.22 (t, 3H, *J* = 7.2 Hz); ^{13}C NMR (100 MHz, DMSO-d_6) δ 165.7, 165.5, 156.6, 153.7, 153.2, 148.7, 148.3, 142.0, 141.6, 140.6, 138.2, 128.6, 127.9, 125.2, 124.8, 121.2, 118.5, 117.3, 109.0, 58.3, 57.0, 55.5, 53.5, 43.5, 40.4, 38.3, 26.0, 25.5, 14.7. MS (ESI) *m/z* 639.20 $(M+H)^+$; HRMS: calcd for $C_{26}H_{29}F_3N_8O_4S_2$ $(M+H)^+$, 639.1778; found 639.1782. mp: 233.1−233.6 °C.

*5.1.16. 1-Ethyl-3-(2'-(3-methyl-3,8-diazabicyclo[3.2.1]octan-8-yl)-5'-(1H-tetrazol-5-yl)-4-(4-(trifluoromethyl)thiazol-2-yl)-[3,3'-bipyridin]-6-yl)urea (**37**):* A mixture of **33** (0.10 g, 0.46 mmol), **12** (0.12 g, 0.5 mmol) and K_2CO_3 (0.21 g, 3 eq) in acetonitrile (20 mL) were stirred at 100 ^{o}C for 16 h. The reaction mixture was diluted with water (20 mL) and extracted with EtOAc (3 x 50 mL). The combined organic layer was washed with water and brine solution, dried over anhydrous Na_2SO_4, filtered, and concentrated under reduced pressure. The crude material was triturated with pentane (10 mL), filtered, and dried to afford 5-bromo-6-(3-methyl-3,8-diazabicyclo[3.2.1]octan-8-yl)nicotinonitrile [0.1 g, MS (ESI) *m/z* 307.03 $(M+H)^+$, 309.03 $(M+2+H)^+$]. Suzuki coupling between this compound and **5** was carried out as per the general procedure to afford 1-(5'-cyano-2'-(3-methyl-3,8-diazabicyclo[3.2.1]octan-

8-yl)-4-(4-(trifluoromethyl)-thiazol-2-yl)-3,3'-bipyridin-6-yl)-3-ethylurea [70 mg, MS (ESI) *m/z* 543.1 $(M+H)^+$] which was dissolved in in DMF (2 mL) and treated with NaN_3 (22 mg, 0.33 mmol) and $AlCl_3$ (cat.) in sealed tube at 120 °C. After 16 h, the reaction mixture was poured into ice-water and the compound was extracted with 10% MeOH in DCM (3 x 20 mL). The combined organic layer was dried over anhydrous Na_2SO_4, filtered, and concentrated under reduced pressure. The crude material was purified by prep-HPLC to afford **37** (3 mg, 11 % yield over three steps) as a gum. ^{1}H NMR (400 MHz, DMSO-d_6) δ 8.92 (d, 1H, *J* = 2.4 Hz), 8.45–8.39 (m, 1H), 8.21 (d, 1H, *J* = 2.0 Hz), 8.12–8.05 (m, 1H), 7.89 (s, 1H), 3.95 (d, 1H, *J* = 5.6 Hz), 3.68 (d, 1H, *J* = 5.6 Hz), 3.38–3.29 (m, 2H), 2.46-2.36 (m, 2H), 2.08 (s, 3H), 1.93 (s, 1H), 1.76–1.62 (m, 3H), 1.48–1.46 (m, 1H), 1.39 (s, 1H), 1.24 (t, 3H, *J* = 7.6 Hz); MS (ESI) *m/z* 586.5 $(M+H)^+$.

*5.1.17. 1-Ethyl-3-(2'-(3-methyl-3,8-diazabicyclo[3.2.1]octan-8-yl)-5'-(5-oxo-4,5-dihydro-1,3,4-oxadiazol-2-yl)-4-(4-(trifluoromethyl)thiazol-2-yl)-[3,3'-bipyridin]-6-yl)urea (**38**):* Suzuki coupling between **27** (1.0 g, 2.8 mmol) and **5** (1.5 g, 4.2 mmol), was carried out as described in the general procedure. The product 6'-(3-ethylureido)-2-(3-methyl-3,8-diazabicyclo[3.2.1]octan-8-yl)-4'-(4-(trifluoromethyl)thiazol-2-yl)-3,3'-bipyridine-5-carboxylate (1.1 g) was dissolved in EtOH (50 mL) and treated with hydrazine hydrate (11 mL). After stirring at 80 ^{o}C for 16 h, the reaction mixture was poured into ice-water and the compound was extracted with EtOAc (3 x 40 mL). The combined organic layer was washed with water and brine solution, dried (anhydrous Na_2SO_4) and evaporated. The crude residue (1.0 g) was dissolved in DCM (200 mL) and treated with carbonyldiimidazole (845 mg, 5.2 mmol) and DIPEA (0.9 mL, 5.2 mmol). After 6 h at room temperature, the reaction mixture was poured into ice-water and the compound was extracted with DCM (3 x 200 mL). The combined organic layer was dried (anhydrous Na_2SO_4) and concentrated. The residue was purified by Prep-HPLC to afford **38** (480 mg, 28 % over three steps). ^{1}H NMR (400 MHz,

DMSO-d_6) δ 12.42 (s, 1H), 9.45 (s, 1H), 8.61 (d, 1H, *J* = 2.4 Hz), 8.50 (s, 1H), 8.37 (s, 1H), 8.22 (s, 1H), 7.88 (d, 1H, *J* = 2.0 Hz), 7.64 (s, 1H), 3.92 (br s, 1H), 3.78 (br s, 1H), 3.24–3.17 (m, 2H), 2.38-2.30 (m, 2H), 2.01 (s, 3H), 1.65-1.51 (m, 4H), 1.35-1.27 (m, 2H), 1.12 (t, 3H, *J* = 7.2 Hz); ^{13}C NMR (100 MHz, DMSO-d_6) δ 166.2, 156.6, 154.4, 153.7, 151.5, 148.9, 143.9, 142.1, 138.8, 136.3, 125.6, 125.5, 119.7, 109.5, 59.8, 58.4, 57.6, 54.8, 44.5, 33.9, 27.7, 26.7, 15.3; MS (ESI) *m/z* 602.2 $(M+H)^+$; HRMS: calcd for $C_{26}H_{26}F_3N_9O_3S$ $(M+H)^+$, 602.1904; found 602.1905. mp: 223.5-225.0 °C.

In a similar manner, **28** (0.7 g) was converted to *tert*-butyl (1-(2-(6-(3-ethylureido)-4-(4-(trifluoromethyl)thiazol-2-yl)pyridin-3-yl)-4-(5-oxo-4,5-dihydro-1,3,4-oxadiazol-2-yl)phenyl)piperidin-4-yl)carbamate **30**, which was dissolved in DCM (4 mL) and treated with TFA (4 mL) at 0 ^{o}C. After stirring at room temperature for 5 h, the reaction mixture was concentrated under reduced pressure and basified using aq.$NaHCO_3$ and extracted with 10% MeOH in DCM (3 x 20 mL). The combined organic layer was dried over anhydrous Na_2SO_4, filtered and concentrated under reduced pressure to afford **39** (8 mg, 1 % over 4 steps). ^{1}H NMR (400 MHz, DMSO-d_6) δ 8.67 (d, 1H, *J* = 2.4 Hz), 8.39 (s, 1H), 8.13 (s, 1H), 8.01 (d, 1H, *J* = 2.0 Hz), 7.86 (s, 1H), 3.39-3.30 (m, 2H), 3.16 (d, 1H, *J* = 12.8 Hz), 2.76 (t, 1H, *J* = 12.0 Hz), 2.59 (s, 1H), 2.45 (t, 1H, *J* = 12.0 Hz), 1.62 (d, 1H, *J* = 11.6 Hz), 1.52 (d, 1H, *J* = 11.6 Hz), 1.28 (s, 2H), 1.23 (t, 3H, *J* = 7.6 Hz), 1.16–1.09 (m, 1H); MS (ESI) *m/z* 576.08 $(M+H)^+$.

Following similar route, **29** was converted to **40** (71 mg, 13% yield over four steps). ^{1}H NMR (400 MHz, DMSO-d_6) δ 9.47 (s, 1H), 8.57 (d, 1H, *J* = 2.2 Hz), 8.49 (d, 1H, *J* = 0.6 Hz), 8.36 (s, 1H), 8.22 (s, 1H), 7.80 (d, 1H, *J* = 2.2 Hz), 7.64 (s, 1H), 4.09-4.07 (m, 1H), 3.66-3.64 (m, 1H), 3.24-3.16 (m, 3H), 3.12-3.05 (m, 1H), 2.54 (s, 1H), 1.61-1.47 (m, 5H), 1.38-1.33 (m, 1H), 1.11 (t, 3H, *J* = 7.1 Hz), 1.00-0.95 (m, 1H); ^{13}C NMR (100 MHz, DMSO-d_6) δ 165.2, 165.1, 157.7, 153.7, 153.2, 151.5, 147.8, 144.3, 142.1, 141.7, 138.5, 136.4,

128.4, 126.8, 125.2, 124.9, 121.2, 118.5, 117.9, 111.9, 109.0, 54.3, 53.3, 41.9, 36.9, 35.2, 33.3, 26.7, 26.1, 14.7. MS (ESI) *m/z* 602.2 $(M+H)^+$; HRMS: calcd for $C_{26}H_{26}F_3N_9O_3S$ $(M+H)^+$, 602.1904; found 602.1906. mp: 335.2-337.9 ^oC.

*5.1.18. 1-(5-Bromo-4-(4-cyclopropylthiazol-2-yl)pyridin-2-yl)-3-ethylurea (**43**):* To a stirred solution of **41** (9.0 g, 29.7 mmol) in acetonitrile (100 mL) was added 2-bromo-1-cyclopropylethan-1-one (8.6 mL, 89.10 mmol) and the mixture was heated to reflux. After 16 h, the reaction mixture was poured into ice-water and extracted with EtOAc (3 x 20 mL). The combined organic layer was washed with water and brine solution, dried (anhydrous Na_2SO_4), concentrated under reduced pressure and purified by column chromatography (silica gel, eluent EtOAc/hexane 3:7) to afford **43** (3.0 g, 30 % yield). ^1H NMR (400 MHz, DMSO-d_6) δ 9.32 (s, 1H), 8.48 (s, 1H), 8.30 (s, 1H), 7.62 (s, 1H), 7.35 (t, 1H, *J* = 5.6 Hz), 3.36-3.14 (m, 2H), 2.21-2.17 (m, 1H), 1.08 (t, 3H, *J* = 7.2 Hz), 1.01-0.96 (m, 2H), 0.91-0.87 (m, 2H). MS (ESI) *m/z* 367.1 $(M+H)^+$, 369.1 $(M+2+H)^+$.

*5.1.19. 1-(4-(4-Cyclopropylthiazol-2-yl)-2'-(3-methyl-3,8-diazabicyclo[3.2.1]octan-8-yl)-5'-(5-oxo-4,5-dihydro-1,3,4-oxadiazol-2-yl)-3,3'-bipyridin-6-yl)-3-ethylurea (**44**):*
To a solution of **43** (350.0 mg, 0.95 mmol) in THF (15 mL) at -78°C was added ^{i}PrMgCl (1.2 mL, 2.3 mmol). After 1 h, n-BuLi (3.3 mL, 5.3 mmol) was added dropwise and allowed to stir at -78°C for 1 h. Trimethyl borate (1.1 mL, 10.197 mmol) was then added and the reaction mixture was allowed to warm to room temperature over 2 h. The reaction mixture was quenched with 1M HCl and stirred for 30 min. The reaction mixture was then concentrated under reduced pressure, then diluted with water and extracted with EtOAc. The combined organic extracts were washed with brine, and dried with $MgSO_4$, concentrated under reduced pressure. The crude product [350 mg, MS (ESI) *m/z* 333.1 $(M+H)^+$] was subjected to Suzuki coupling with **27** (135 mg, 0.38 mmol) under conditions mentioned in the general procedure to afford 17.5 mg of ethyl 4'-(4-cyclopropylthiazol-2-yl)-6'-(3-

ethylureido)-2-(3-methyl-3,8-diazabicyclo[3.2.1]octan-8-yl)-[3,3'-bipyridine]-5-carboxylate [MS (ESI) *m/z* 562.2 $(M+H)^+$] which was dissolved in EtOH (10 mL) and treated with hydrazine hydrate (1 mL) at 80°. After 16 h, the reaction mixture was concentrated and the residue was diluted with water and extracted with EtOAc. Organic layer was dried (Na_2SO_4), evaporated and the residue [MS (ESI) *m/z* 548.2 $(M+H)^+$] was re-dissolved in DCM (3 mL) and treated with carbonyldiimidazole (12.43 mg, 0.077 mmol) and diisopropylethylamine (13.4 µL, 0.077 mmol). After 16 h at room temperature the reaction mixture was diluted with water, and extracted with DCM. The combined organic layers were washed with brine, dried ($MgSO_4$) and concentrated under reduced pressure. The residue was purified by reversed phase preparative HPLC (C18, eluent MeCN, water, formic acid 0.1%) to afford **44** (2.8 mg, 5 % yield over four steps). ^{1}H NMR (400 MHz, DMSO-d_6) δ 12.39 (s, 1H), 9.37 (s, 1H), 8.53 (d, 1H, *J* =2.0 Hz), 8.24 (s, 1H), 8.11 (s, 1H), 7.71-7.66 (m, 2H), 7.34 (s, 1H), 3.92 (s, 2H), 3.32-3.19 (m, 2H), 2.35-2.31 (m, 2H), 2.01-1.97 (m, 5H), 1.66-1.54 (m, 4H), 1.39 (br s, 1H), 1.10 (t, 3H, *J* =7.2 Hz), 0.84-0.81 (m, 2H), 0.67-0.58 (m, 2H); ^{13}C NMR (100 MHz, DMSO-d_6) δ 162.3, 158.7, 157.4, 154.4, 154.3, 153.6, 152.7, 148.6, 144.8, 139.9, 136.9, 124.9, 120.1, 114.5, 110.9, 109.5, 59.4, 58.6, 56.3, 55.0, 44.6, 33.9, 27.4, 26.9, 15.3, 11.6, 7.9. MS (ESI) *m/z* 574.2 $(M+H)^+$; HRMS: calcd for $C_{28}H_{31}N_9O_3S$ $(M+H)^+$, 574.2343; found 574.2343. mp: 220.0-223.0 °C.

5.2. Protein expression, purification and x-ray crystallography

Recombinant *S. pneumoniae* ParE ATPase domain (residues 1-226) was expressed and purified as described in literature [32].

5.2.1. E.coli GyrB purification method: To produce the active domain of GyraseB of *E. coli*, cDNA encoding residues 1-220 of GyraseB was amplified using the E. coli genome as a template. The cDNA of GyraseB was cloned into the NdeI and XhoI sites of the pET29b. The resulting plasmid encodes the active domain of GyraseB with an extra tag containing 8

residues (LEHHHHHH) at the C-terminus to aid in protein purification. To express GyraseB from *E. coli* for NMR studies, the plasmid was transformed in *E. coli* (BL21DE3) competent cells and plated onto a LB plate containing kanamicin. The protein was expressed and purified using the similar protocol to that described previously [32]. Briefly, several colonies were inoculated in 20 ml of M9 medium and cultured at 37 °C overnight with shaking. The overnight culture was then transferred into 1 litre of M9 medium supplied with 30 µg/ml kanamycin and 2 g/l of ^{13}C-Glucose and 1 g/l ^{15}N-NH_4Cl. Protein was induced for overnight at 18 °C by adding β-D-1-thiogalactopyranoside to 1 mM. The recombinant protein was then purified using a gravity column with nitrilotriacetic acid saturated with nickel (Ni^{2+}-NTA) resin, followed with a further purification with gel filtration. GyrB was prepared in a buffer containing 20 mM sodium phosphate, pH 6.5, 80 mM KCl, 2 mM DTT and 0.5 mM EDTA to prevent sample precipitation. For crystallization study, the *E. coli* cells were grown in LB medium and purified in a buffer that contained 20 mM Tris-HCL, 150 mM NaCl and 1 mM DTT.

Apo ParE crystals were grown from 0.2 M Sodium Acetate and 18-22% PEG3350 by hanging drop vapor diffusion method. Protein (2 µL, 9 mg/mL) and mother liquor (2 µL) were set up at room temperature. Long thin, plate-like crystals appeared after 2-3 days and grew to full size within a week.

Compound **38** was co-crystallized with ParE by addition of 1:5 Molar ratio in excess of compound. Crystals grew by hanging drop vapour diffusion method in 0.2 M Ammonium citrate buffer with 15-22 % PEG3350 at room temperature. Rod-like crystals appeared within 3 days and grew to full size within a week. Crystals belong to space group $P12_11$ with two molecule in an asymmetric unit. All crystals were cryoprotected in solution of 4.5 µL mother liquor and 1 µL 2,3-butanediol. Crystals were flash frozen in liquid N_2 prior to X-ray diffraction data collection.

X-ray diffraction data was collected at 2173uC on a Bruker X8 PROTEUM system consist of a MICROSTAR micro-focus X-ray generator, a PLATIMUM 135 CCD detector and a 4-circle KAPPA goniometer. Diffraction data was integrated and scaled using the Bruker PROTEUM2 program suites (Bruker AXS inc., Bruker AXS (2009), PROTEUM2, Version 2009 Bruker AXS Inc., Madison, Wisconsin, USA). The ParE structures were solved by molecular replacement with structure 4EMV as search model. GyrB structures were solved by using 1KZN as search model. Molecular replacement was performed with Phaser [33] and model refined by Phenix._ENREF_30 [34] Compound restrained files were generated using ProDRG [35]. Model building and refinement was conducted using COOT [36] and Phenix refine [37] Table 7 gives a summary of the data collection and refinement statistics.

Table 7: X-ray Data Processing and Refinement Statistics

Compound	**38**
Protein	ParE
PDB ID	5YIG
Data collection	
Space group	$P12_11$
Cell dimensions	
a, *b*, *c* (Å)	43.39, 61.98, 84.82
α, β, γ (°)	90, 99, 90
Resolution (Å)	35.93-2.8 (2.9-2.8) [1]
R_{merge} [2]	0.179 (0.474)
Completeness (%)	99.51 (99.64)
Mean I/sI	5.72 (2.09)
Multiplicity	2.80 (2.90)
Refinement	
R_{work}/R_{free} [3]	0.206/0.255

No. atoms	
Protein	3029
Ligand	84
Solvent/ions	6
Average B values (Å^2)	
Protein	25.5
Ligand	29.2
Solvent/ions	16.1
R.m.s. deviations	
Bond lengths	0.005
Bond angles	0.99

5.2.2. MIC determination: MIC values were determined by the broth microdilution method in accordance with the Clinical and Laboratory Standards Institute (CLSI) guidelines. In brief, bacterial suspensions were adjusted to 1 × l0^6 colony-forming units (CFU)/mL in cation adjusted Mueller−Hinton broth (Beckton Dickinson).

An inoculum volume of 50 μL was added to wells containing 50 μL of 2-fold serially diluted compounds. The final concentration of DMSO is 2.5% v/v. All the plates were incubated at 35 °C, 140 rpm for 24 h. Following incubation, the lowest concentration of the drug that prevented visible growth as determined by OD_{600} nm was recorded as the MIC.

5.3. pK_a Determination. pK_a values were determined on a Sirius DTu machine (Sirius Analytical Instruments) by a Gold Standard pH metric assay in triplicate.

Notes

The authors declare no competing financial interest.

Author contributions

The manuscript was written through contributions of all authors. All authors have given approval to the final version of the manuscript.

Acknowledgments

We thank Alex Matter (Experimental Therapeutics Centre), Manos Perros, Ruben Tommasi, Gunther Kern and Thomas Keating (AstraZeneca) for their support and constructive comments.

Funding

This work was funded by the Agency for Science, Technology and Research (A*STAR) Biomedical Research Council core fund.

Appendix A. Supplementary data

Supplementary data related to this manuscript (IC_{50} values with standard error, GI_{50} of compounds against A549 cells and details of bacterial strains used in MIC_{90} determination) can be downloaded online.

PDB code: PDB ID 5YIG. Authors will release atomic coordinates and experimental data upon article publication.

References:

[1] Pendleton, J. N.; Gorman, S. P.; Gilmore, B. F., Clinical relevance of the ESKAPE pathogens. Expert. Rev. *Anti Infect. Ther.* **2013**, *11*, 297-308.

[2] Piddock, L. J., The crisis of no new antibiotics-what is the way forward? *Lancet Infect. Dis.* **2012**, *12*, 249-53.

[3] Boucher, H. W.; Talbot, G. H.; Benjamin, D. K., Jr.; Bradley, J.; Guidos, R. J.; Jones, R. N.; Murray, B. E.; Bonomo, R. A.; Gilbert, D.; Infectious Diseases Society of, A., 10 x '20 Progress--development of new drugs active against gram-negative bacilli: an update from the Infectious Diseases Society of America. *Clinical infectious diseases: an official publication of the Infectious Diseases Society of America* **2013**, *56*, 1685-94.

[4] Ceftolozane/Tazobactam (Zerbaxa) - a new intravenous antibiotic. *Med. Lett. Drugs Ther.* **2015**, *57*, 31-3.

[5] Ceftazidime/Avibactam (Avycaz) - a new intraveneous antibiotic. *Med. Lett. Drugs Ther.* **2015**, *57*, 79-80.

[6] Queenan, A. M.; Bush, K., Carbapenemases: the versatile beta-lactamases. *Clin. Microbiol. Rev.* **2007**, *20*, 440-58.

[7] Ehmann, D. E.; Jahic, H.; Ross, P. L.; Gu, R. F.; Hu, J.; Durand-Reville, T. F.; Lahiri, S.; Thresher, J.; Livchak, S.; Gao, N.; Palmer, T.; Walkup, G. K.; Fisher, S. L., Kinetics of avibactam inhibition against Class A, C, and D beta-lactamases. *J. Biol. Chem.* **2013**, *288*, 27960-71.

[8] Lagace-Wiens, P.; Walkty, A.; Karlowsky, J. A., Ceftazidime-avibactam: an evidence-based review of its pharmacology and potential use in the treatment of Gram-negative bacterial infections. *Core Evid.* **2014**, *9*, 13-25.

[9] Silver, L. L., Multi-targeting by monotherapeutic antibacterials. *Nat. Rev. Drug Discov.* **2007**, *6*, 41-55.

[10] Brvar, M.; Perdih, A.; Renko, M.; Anderluh, G.; Turk, D.; Solmajer, T., Structure-based discovery of substituted 4,5'-bithiazoles as novel DNA gyrase inhibitors. *J. Med. Chem.* **2012**, *55*, 6413-26.

[11] Ehmann, D. E.; Lahiri, S. D., Novel compounds targeting bacterial DNA topoisomerase/DNA gyrase. *Curr. Opin. Pharmacol.* **2014**, *18*, 76-83.

[12] Musicki, B.; Periers, A.-M.; Piombo, L.; Laurin, P.; Klich, M.; Dupuis-Hamelin, C.; Lassaigne, P.; Bonnefoy, A., Noviose mimics of the coumarin inhibitors of gyrase B. *Tet. Lett.* **2003**, *44*, 9259-9262.

[13] Sherer, B. A.; Hull, K.; Green, O.; Basarab, G.; Hauck, S.; Hill, P.; Loch, J. T., 3rd; Mullen, G.; Bist, S.; Bryant, J.; Boriack-Sjodin, A.; Read, J.; DeGrace, N.; Uria-Nickelsen, M.; Illingworth, R. N.; Eakin, A. E., Pyrrolamide DNA gyrase inhibitors: optimization of antibacterial activity and efficacy. *Bioorg. Med. Chem. Lett.* **2011**, *21*, 7416-20.

[14] Shirude, P. S.; Madhavapeddi, P.; Tucker, J. A.; Murugan, K.; Patil, V.; Basavarajappa, H.; Raichurkar, A. V.; Humnabadkar, V.; Hussein, S.; Sharma, S.; Ramya, V. K.; Narayan, C. B.; Balganesh, T. S.; Sambandamurthy, V. K., Aminopyrazinamides: novel and specific GyrB inhibitors that kill replicating and nonreplicating Mycobacterium tuberculosis. *ACS Chem. Biol.* **2013**, *8*, 519-23.

[15] Stokes, N. R.; Thomaides-Brears, H. B.; Barker, S.; Bennett, J. M.; Berry, J.; Collins, I.; Czaplewski, L. G.; Gamble, V.; Lancett, P.; Logan, A.; Lunniss, C. J.; Peasley, H.; Pommier, S.; Price, D.; Smee, C.; Haydon, D. J., Biological evaluation of benzothiazole ethyl urea inhibitors of bacterial type II topoisomerases. *Antimicrob. Agents Chemother.* **2013**, *57*, 5977-86.

[16] Tari, L. W.; Li, X.; Trzoss, M.; Bensen, D. C.; Chen, Z.; Lam, T.; Zhang, J.; Lee, S. J.; Hough, G.; Phillipson, D.; Akers-Rodriguez, S.; Cunningham, M. L.; Kwan, B. P.; Nelson, K. J.; Castellano, A.; Locke, J. B.; Brown-Driver, V.; Murphy, T. M.; Ong, V. S.; Pillar, C. M.; Shinabarger, D. L.; Nix, J.; Lightstone, F. C.; Wong, S. E.; Nguyen, T. B.; Shaw, K. J.;

Finn, J., Tricyclic GyrB/ParE (TriBE) inhibitors: a new class of broad-spectrum dual-targeting antibacterial agents. *PloS One* **2013**, *8*, e84409.

[17] Tari, L. W.; Trzoss, M.; Bensen, D. C.; Li, X.; Chen, Z.; Lam, T.; Zhang, J.; Creighton, C. J.; Cunningham, M. L.; Kwan, B.; Stidham, M.; Shaw, K. J.; Lightstone, F. C.; Wong, S. E.; Nguyen, T. B.; Nix, J.; Finn, J., Pyrrolopyrimidine inhibitors of DNA gyrase B (GyrB) and topoisomerase IV (ParE). Part I: Structure guided discovery and optimization of dual targeting agents with potent, broad-spectrum enzymatic activity. *Bioorg. Med. Chem. Lett.* **2013**, *23*, 1529-36.

[18] Trzoss, M.; Bensen, D. C.; Li, X.; Chen, Z.; Lam, T.; Zhang, J.; Creighton, C. J.; Cunningham, M. L.; Kwan, B.; Stidham, M.; Nelson, K.; Brown-Driver, V.; Castellano, A.; Shaw, K. J.; Lightstone, F. C.; Wong, S. E.; Nguyen, T. B.; Finn, J.; Tari, L. W., Pyrrolopyrimidine inhibitors of DNA gyrase B (GyrB) and topoisomerase IV (ParE), Part II: development of inhibitors with broad spectrum, Gram-negative antibacterial activity. *Bioorg. Med. Chem. Lett.* **2013**, *23*, 1537-43.

[19] Bisacchi, G. S.; Manchester, J. I., A New-Class Antibacterial—Almost. Lessons in Drug Discovery and Development: A Critical Analysis of More than 50 Years of Effort toward ATPase Inhibitors of DNA Gyrase and Topoisomerase IV. *ACS Infect. Dis.* **2015**, *1*, 4-41.

[20] Panchaud, P.; Bruyère, T.; Blumstein, A. C.; Bur, D.; Chambovey, A.; Ertel, E. A.; Gude, M.; Hubschwerlen, C.; Jacob, L.; Kimmerlin, T.; Pfeifer, T.; Prade, L.; Seiler, P.; Ritz, D.; Rueedi, G., Discovery and Optimization of Isoquinoline Ethyl Ureas as Antibacterial Agents. *J. Med. Chem.* **2017**, *20*, 3755-3775.

[21] Silver, L. L., Challenges of antibacterial discovery. *Clin. Microbiol. Rev.* **2011**, *24*, 71-109.

[22] Pages, J. M.; James, C. E.; Winterhalter, M., The porin and the permeating antibiotic: a selective diffusion barrier in Gram-negative bacteria. *Nat. Rev. Microbiol.* **2008**, *6*, 893-903.

[23] Khodursky, A. B.; Peter, B. J.; Schmid, M. B.; DeRisi, J.; Botstein, D.; Brown, P. O.; Cozzarelli, N. R., Analysis of topoisomerase function in bacterial replication fork movement: use of DNA microarrays. *Proc. Natl. Acad. Sci. U. S. A.* **2000**, *97*, 9419-24.

[24] Bellon, S.; Parsons, J. D.; Wei, Y.; Hayakawa, K.; Swenson, L. L.; Charifson, P. S.; Lippke, J. A.; Aldape, R.; Gross, C. H., Crystal Structures of Escherichia coli Topoisomerase IV ParE Subunit (24 and 43 Kilodaltons): a Single Residue Dictates Differences in Novobiocin Potency against Topoisomerase IV and DNA Gyrase. *Antimicrob. Agents Chemother.* **2004**, *48*, 1856-1864.

[25] Manchester, J. I.; Buurman, E. T.; Bisacchi, G. S.; McLaughlin, R. E., Molecular determinants of AcrB-mediated bacterial efflux implications for drug discovery. *J. Med. Chem.* **2012**, *55*, 2532-7.

[26] O'Shea, R.; Moser, H. E., Physicochemical properties of antibacterial compounds: implications for drug discovery. *J. Med. Chem.* **2008**, *51*, 2871-8.

[27] Basarab, G. S.; Manchester, J. I.; Bist, S.; Boriack-Sjodin, P. A.; Dangel, B.; Illingworth, R.; Sherer, B. A.; Sriram, S.; Uria-Nickelsen, M.; Eakin, A. E., Fragment-to-hit-to-lead discovery of a novel pyridylurea scaffold of ATP competitive dual targeting type II topoisomerase inhibiting antibacterial agents. *J. Med. Chem.* **2013**, *56*, 8712-35.

[28] Richter, M. F.; Drown, B. S.; Riley, A. P.; Garcia, A.; Shirai, T.; Svec, R. L.; Hergenrother, P. J., Predictive compound accumulation rules yield a broad-spectrum antibiotic. *Nature* **2017**, *545*, 299-304.

[29] Li, Y.; Wong, Y. L.; Ng, F. M.; Liu, B.; Wong, Y. X.; Poh, Z. Y.; Liu, S.; Then, S. W.; Lee, M. Y.; Ng, H. Q.; Huang, Q.; Hung, A. W.; Cherian, J.; Hill, J.; Keller, T. H.; Kang, C., Escherichia coli Topoisomerase IV E Subunit and an Inhibitor Binding Mode Revealed by NMR Spectroscopy. *J. Biol. Chem.* **2016**, *291*, 17743-53.

[30] Li, Y.; Wong, Y. X.; Poh, Z. Y.; Wong, Y. L.; Lee, M. Y.; Ng, H. Q.; Liu, B.; Hung, A. W.; Cherian, J.; Hill, J.; Keller, T. H.; Kang, C., NMR structural characterization of the N-terminal active domain of the gyrase B subunit from Pseudomonas aeruginosa and its complex with an inhibitor. *FEBS Lett.* **2015**, *589*, 2683-9.

[31] Kim, A.; Kutschke, A.; Ehmann, D. E.; Patey, S. A.; Crandon, J. L.; Gorseth, E.; Miller, A. A.; McLaughlin, R. E.; Blinn, C. M.; Chen, A.; Nayar, A. S.; Dangel, B.; Tsai, A. S.; Rooney, M. T.; Murphy-Benenato, K. E.; Eakin, A. E.; Nicolau, D. P., Pharmacodynamic Profiling of a Siderophore-Conjugated Monocarbam in Pseudomonas aeruginosa: Assessing the Risk for Resistance and Attenuated Efficacy. *Antimicrob. Agents Chemother.* **2015**, *59*, 7743-52.

[32] Murphy-Benenato, K. E.; Bhagunde, P. R.; Chen, A.; Davis, H. E.; Durand-Reville, T. F.; Ehmann, D. E.; Galullo, V.; Harris, J. J.; Hatoum-Mokdad, H.; Jahic, H.; Kim, A.; Manjunatha, M. R.; Manyak, E. L.; Mueller, J.; Patey, S.; Quiroga, O.; Rooney, M.; Sha, L.; Shapiro, A. B.; Sylvester, M.; Tan, B.; Tsai, A. S.; Uria-Nickelsen, M.; Wu, Y.; Zambrowski, M.; Zhao, S. X., Discovery of efficacious Pseudomonas aeruginosa-targeted siderophore-conjugated monocarbams by application of a semi-mechanistic pharmacokinetic/pharmacodynamic model. *J. Med. Chem.* **2015**, *58*, 2195-205.

[33] Kale, M. G.; Raichurkar, A.; P, S. H.; Waterson, D.; McKinney, D.; Manjunatha, M. R.; Kranthi, U.; Koushik, K.; Jena, L.; Shinde, V.; Rudrapatna, S.; Barde, S.; Humnabadkar, V.; Madhavapeddi, P.; Basavarajappa, H.; Ghosh, A.; Ramya, V. K.; Guptha, S.; Sharma, S.; Vachaspati, P.; Kumar, K. N.; Giridhar, J.; Reddy, J.; Panduga, V.; Ganguly, S.; Ahuja, V.; Gaonkar, S.; Kumar, C. N.; Ogg, D.; Tucker, J. A.; Boriack-Sjodin, P. A.; de Sousa, S. M.; Sambandamurthy, V. K.; Ghorpade, S. R., Thiazolopyridine ureas as novel antitubercular agents acting through inhibition of DNA Gyrase B. *J. Med. Chem.* **2013**, *56*, 8834-48.

[34] McCoy, A. J.; Grosse-Kunstleve, R. W.; Adams, P. D.; Winn, M. D.; Storoni, L. C.; Read, R. J., Phaser crystallographic software. *J. Appl. Crystallogr.* **2007**, *40*, 658-674.

[35] Adams, P. D.; Afonine, P. V.; Bunkoczi, G.; Chen, V. B.; Davis, I. W.; Echols, N.; Headd, J. J.; Hung, L. W.; Kapral, G. J.; Grosse-Kunstleve, R. W.; McCoy, A. J.; Moriarty, N. W.; Oeffner, R.; Read, R. J.; Richardson, D. C.; Richardson, J. S.; Terwilliger, T. C.; Zwart, P. H., PHENIX: a comprehensive Python-based system for macromolecular structure solution. *Acta Crystallogr. D Biol. Crystallogr.* **2010**, *66*, 213-21.

[36] Schuttelkopf, A. W.; van Aalten, D. M., PRODRG: a tool for high-throughput crystallography of protein-ligand complexes. *Acta Crystallogr. D Biol. Crystallogr.* **2004**, *60*, 1355-63.

[37] Emsley, P.; Cowtan, K., Coot: model-building tools for molecular graphics. *Acta Crystallogr. D Biol. Crystallogr.* **2004**, *60*, 2126-32.

[38] Afonine, P. V.; Grosse-Kunstleve, R. W.; Echols, N.; Headd, J. J.; Moriarty, N. W.; Mustyakimov, M.; Terwilliger, T. C.; Urzhumtsev, A.; Zwart, P. H.; Adams, P. D., Towards automated crystallographic structure refinement with phenix.refine. *Acta Crystallogr. D Biol. Crystallogr.* **2012**, *68*, 352-67.

Highlights:

- Potent dual inhibitors of Gram-negative GyraseB and ParE enzymes has been identified.
- Balancing the basicity and acidity of the groups lead to compounds with good permeability as illustrated by their MIC against Gram-negative pathogens such as *E.coli* and *P.aeruginosa* (2.40 -1.1 µg/mL).
- Compounds exhibit broad-spectrum activity and 2 - 8 µg/mL MIC_{90} against *P.aeruginosa* and *A.baumannii*.